Centrifuge modelling on failure behavior of the slope with anti-slide piles under drawdown condition

Sujia Liu, F. Luo, and G. Zhang

State Key Laboratory of Hydroscience and Engineering, Tsinghua University, China.

ABSTRACT

Decrease of water level is an important reason for slope failure. Anti-slide pile is an effective approach for slope reinforcement. Centrifuge model tests were conducted to study the behavior of slope with anti-slide piles under drawdown condition. The failure mechanism and effect of anti-slide piles were discussed based on the displacement measurement. Anti-slide piles rotated around the tips of piles during drawdown. The slope failure occurred in the left part of anti-slide piles with a curved slip surface. The slip surface developed from the top of the slope to the anti-slide piles under drawdown condition. The instability of anti-slide piles occurred before the slip surface developed there. The local failure of the slope was caused by deformation localization and led to more remarkable deformation localization, indicating a significant coupling effect between deformation localization and failure processes under drawdown condition.

Keywords: slope; anti-slide pile; drawdown; failure; centrifugal model test

1 INTRODUCTION

Anti-slide piles are in common use to reinforce slopes. However, the reinforcement effect of anti-piles has not been reasonably evaluated for the slopes near the rivers and reservoirs that experience frequent changes in water level. It is important to analyze the failure mechanism of the slope with anti-slide piles under drawdown condition.

Centrifuge model tests have been widely used to simulate the deformation and failure behavior of the slopes considering different conditions, such as different climatic conditions, excavation conditions and earthquake conditions (Hudacsek et al. 2009; Sommers and Viswanadham 2009; Li et al. 2011; Wang and Zhang 2014).

This paper conducted centrifuge model tests to investigate the deformation and failure behavior of the slope with anti-slide piles under drawdown condition.

2 TEST

2.1 Device

The centrifuge at Tsinghua University was used to conduct the centrifuge model test with a maximum acceleration of 250 g and a capacity of 50 g-ton. The test used a model container with a transparent organic glass on the lateral side to observe the deformation of the slope and the movement of the anti-slide piles. It was designed with a length of 600 mm, a width of 200 mm and a height of 360 mm (Fig. 1).

The change of water level could be simulated using a water variation device (Luo and Zhang 2016).

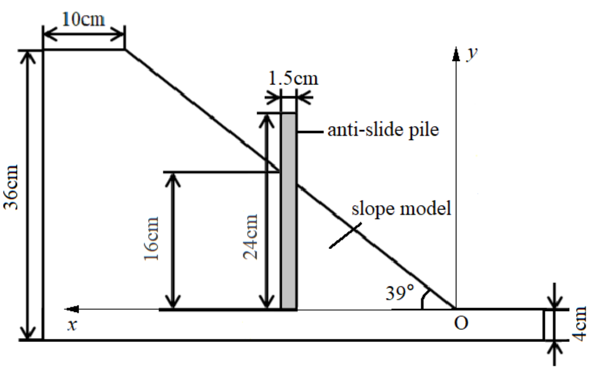

(a) Orthographic view

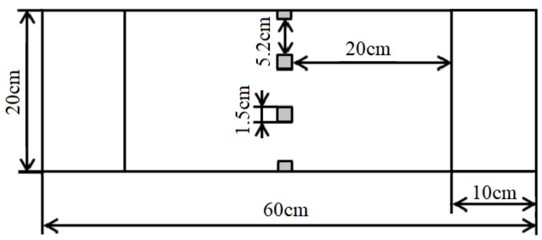

(b) Overhead view

Fig. 1. Schematic view of the slope model.

2.2 Model

A kind of silty clay was used for the slope model, of which the height was 32 cm. Four anti-slide piles with a length of 24 cm were inserted in a row in the slope with an insertion depth of 16 cm and a horizontal distance of 20 cm to the foot of the slope. The side length of each anti-slide pile was 1.5 cm (Fig. 1).

The dry density of the slope was 1.55 g/cm³ and its initial water content was 18%. The shear strength parameters of the soil were 33 kPa in cohesion and 27° in internal frictional angle. The permeability coefficient of the soil was approximately 10 cm/s. It was compacted layer by layer and the thickness of each layer was 40mm. The angle of the slope was 39°. To observe and determine the displacement of the soil more accurately, white particles were evenly placed on the lateral side of the slope model. A camera was placed in front of the transparent organic glass to take images for analysis.

2.3 Procedure

First, raise centrifugal acceleration from 1 g to 10 g, 20g, 30g, 40 g, 50 g step by step. During this process, wait and observe 10 min to confirm the deformation of the slope was stable and apply the next load.

Second, raise the water level from 0 mm to 60 mm, 120 mm, 180 mm, 240 mm. Keep observing the deformation of the slope until the deformation of the slope was stable.

Finally, the water level decreased from 240 mm to 0 mm, which caused the failure of slope and the instability of anti-slide piles (Fig. 2). Then the test was ended.

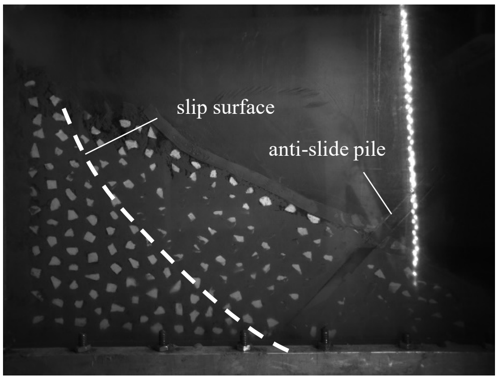

Fig. 2. Photograph of the slope model.

2.4 Measurements

Pictures and videos were taken by the camera to record the whole process of slope and anti-slide piles during the test. Then the position of every marked point at any time could be determined according to the images (Zhang et al. 2009). Thus, the displacement field of the slope could be obtained. A Cartesian coordinate was set up to show the slope displacement more intuitively (Fig. 1). The origin of the Cartesian coordinate was at the foot of slope and the positive direction of the x-axis and y-axis was rightwards and upwards. According to the similarity ratio of centrifuge model test, the prototype displacement is 50 times that of the model.

3 OBSERVATION

It can be seen there was an obvious slip surface and anti-slide piles fell down after test in Figure 2. The slip surface was curved and it ran from the top of the slope to the tips of anti-slide piles.

Figure 3 shows the horizontal displacement along the depth slope after slope failure. The left, middle and right figures show the horizontal displacements of the left part of the slope, anti-slide piles and the right part of the slope. It can be seen that the displacements of both parts increased with height. The horizontal displacements of left part grew rapidly in specific points; their variations were not linear. Therefore, a slip surface occurred in the left part. By contrast, the vertical distributions of horizontal displacements of the right part were nearly linear, whose inclination were close to that of the anti-slide piles. Therefore, it can be assumed that the cause for the deformation of the right part was the extrusion from anti-slide piles. This shows different slope failure modes of the left part and right part of the slope.

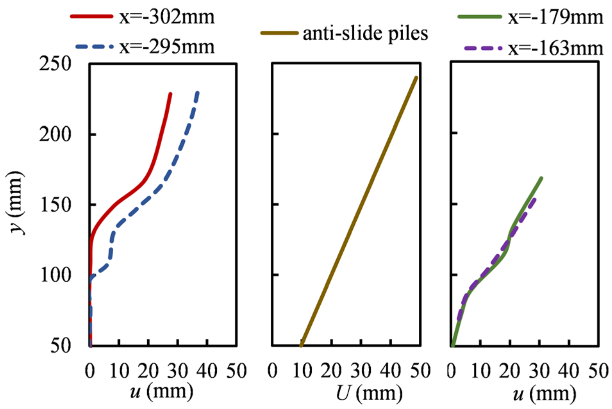

Fig. 3. Horizontal displacement along the depth slope after slope failure. *h*, the water level; *u*, the horizontal displacements of the points on the slope; *U*, the horizonal displacements of anti-slide piles.

The point couple is composed of a pair of adjacent points on different sides of the slip surface. The relative displacement of the point couple can be decomposed to the tangential direction of the slip surface and the normal direction. The positions of five point couples are shown in Figure 4.

Figure 5 shows histories of relative displacement of three point couples. They increased continuously as the water level decreased. It can be seen that both the relative displacements tangential and normal to the slip surface increased slowly at the beginning of drawdown. Whereas, they increased rapidly from a certain moment, which could be regarded as the moment when the local failure occurred. The relative displacements tangential to the slip surface were greater than the relative displacement normal to the slip surface, which indicated that shear failure occurred in the slope. The water level was used to record the moment when the local failure occurred. The local failure moments of point couples are marked in Figure 4. It can be seen that the slip surface developed from the top of the slope to the bottom.

Anti-slide piles can be seen as rigid bodies and was discovered that rotated around the tips of piles. Figure 6 shows the history of rotation angle of the anti-slide piles. It can be seen that the rotation angle grew up as the water level decreased. The rotation angle increased rapidly from a certain moment at which the instability of anti-slide piles appeared. The water level of that moment is also marked in Figure 4. It can be seen that the instability of anti-slide piles occurred before the slip surface of the slope developed there.

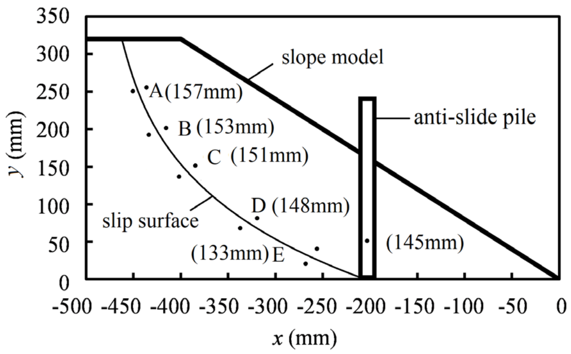

Fig. 4. Failure process of the slip surface.

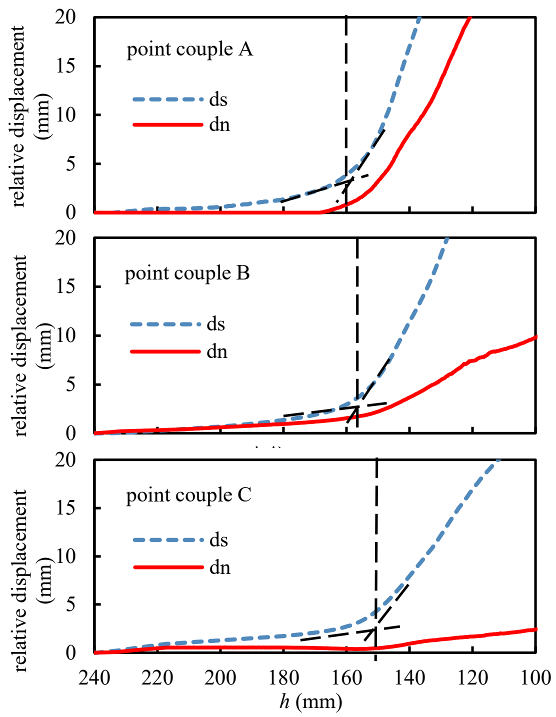

Fig. 5. The relative displacement histories of point couples (locations shown in Fig. 4). *ds*, the relative displacement tangential to the slip surface; *dn*, the relative displacement normal to the slip surface; *h*, the water level.

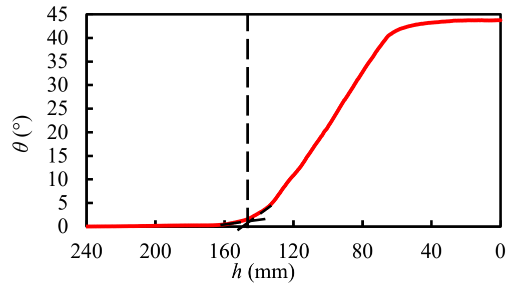

Fig. 6. History of rotation angle of the anti-slide piles. *h*, the water level; θ, the angle of rotation.

4 FAILURE MECHANISM

Figure 7 shows the horizontal distributions of the horizontal displacements before and after slope failure. The dashed lines represent the position of slip surface in the elevation. It can be seen that the displacement exhibited a non-uniform distribution. In a certain area, the displacement changed more significant, which implied that there was an obvious deformation concentration. Thus, the horizontal distributions of the gradient of horizontal displacements were analyzed to illustrate the deformation characteristics of the slope.

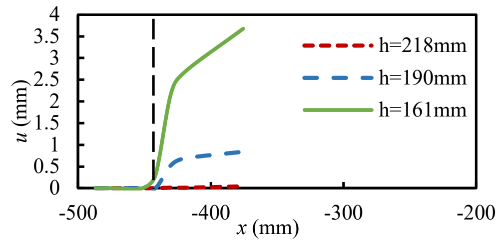

(a) before slope failure

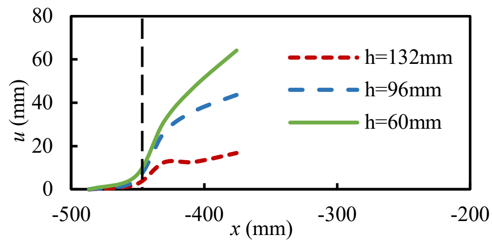

(b) after slope failure

Fig. 7. Horizontal distributions of the horizontal displacements. *h*, the water level; *u*, the horizontal displacements.

Figure 8 shows the horizontal distribution of the horizontal displacement gradient before slope failure. There were significant deformations and uneven distribution in the slope. The deformation increased as the water level decreased and emerge a localization. The deformation localization was limited within a zone and the extent increased during drawdown. It should be noted that the slip surface, outlined using a dashed line in Figure 8, occurred exactly in the deformation localization area as the localization developed to an extent. It can be concluded that the decline of water level led to deformation localization of the slope that developed and induced the local failure there.

Figure 9 shows the horizontal distribution of the horizontal displacement gradient after slope failure. It can be seen there was a more significant peak near the slip surface. This indicated that the local failure led to more remarkable deformation localization. Therefore, the failure mechanism of the slope could be described by the significant coupling processes between the deformation localization and local failure under drawdown condition.

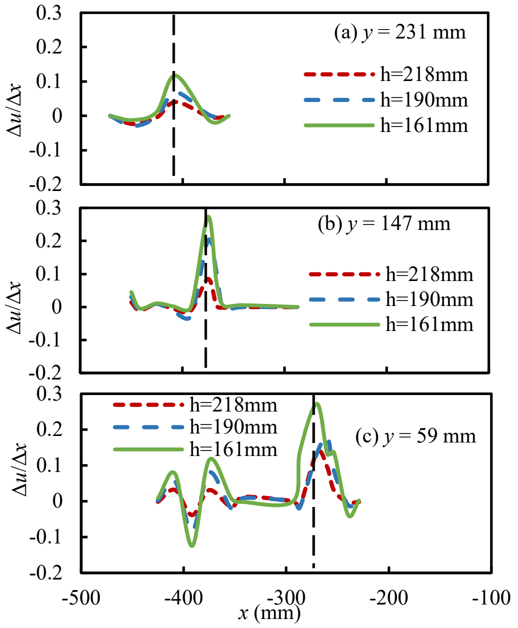

Fig. 8. Horizontal distribution of the horizontal displacement gradient before slope failure. *h*, the water level; *u*, the horizontal displacements.

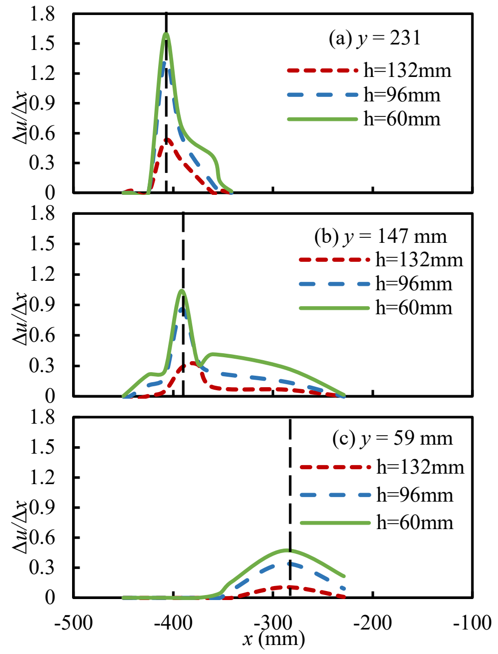

Fig. 9. Horizontal distribution of the horizontal displacement gradient after slope failure. *h*, the water level; *u*, the horizontal displacements.

5 CONCLUSION

(1) Anti-slide piles rotated around the tips of piles during drawdown. The slope failure occurred in the left part of anti-slide piles with a curved slip surface.

(2) The slip surface developed from the top of the slope to the anti-slide piles under drawdown condition. The instability of anti-slide piles occurred before the slip surface developed there.

(3) There was a significant coupling effect between deformation localization and failure processes of the slope. Drawdown led to deformation localization that developed to induce the local failure. The local failure led to more remarkable deformation localization.

ACKNOWLEDGEMENTS

The study is supported by Training Program of Innovation and Entrepreneurship for Undergraduates (No. 201810003B001) and Tsinghua University Initiative Scientific Research Program.

REFERENCES

Hudacsek P, Bransby MF, Hallett PD, Bengough AG (2009) Centrifuge modelling of climatic effects on clay embankments. Proc ICE-Eng Sustainability 162 (2): 91-100.

Li M, Zhang G, Zhang JM, Lee CF (2011) Centrifuge model tests on a cohesive soil slope under excavation conditions. Soils and Foundations 51(5): 801-812.

Luo Fangyue, Zhang Ga. Progressive failure behavior ofcohesive soil slopes under water drawdown conditions. Environmental Earth Sciences, 2016, 75 (11): 973.

Luo Fangyue, Zhang Jiahao, Zhang Zefan, Zhang Ga. Centrifuge model test on failure of soil slope under drawdown of water level. China Civil Engineering Journal, 2017, 50(03):108-114.

Sommers AN, Viswanadham BVS (2009) Centrifuge model tests on the behavior of strip footing on geotextile-reinforced slopes. Geotextiles and Geomembranes 27(6): 497-505.

Wang LP, Zhang G (2014) Centrifuge model test study on pile reinforcement behavior of cohesive soil slopes under earthquake conditions. Landslides 11(2): 213-223.

Zhang G, Hu Y, Zhang JM (2009). New image analysis-based displacement-measurement system for geotechnical centrifuge modeling tests. Measurement 42(1): 87-96.